

Fabrication and assembly of the gyrotron multi-stage depressed collector prototype at KIT

Benjamin Ell^{1,*}, Chuanren Wu¹, Lukas Feuerstein¹, Gerd Gantenbein¹, Stefan Illy¹, Tobias Ruess¹, Tomasz Rzesnicki¹, Sebastian Stanculovic¹, Manfred Thumm¹, Jörg Weggen¹, and John Jelonnek¹

¹Institute for Pulsed Power and Microwave Technology (IHM), Karlsruhe Institute of Technology (KIT), Kaiserstraße 12, 76131 Karlsruhe, Germany

Abstract. In this paper details of the fabrication and assembly of the first Multi-stage Depressed Collector (MDC) prototype developed at KIT for megawatt-class gyrotrons are presented. Utilizing the $E \times B$ drift concept for electron trajectory separation, the cylindrical Short-Pulse (SP) MDC prototype features a design compatible with applications in different fusion gyrotrons at KIT, for W7-X, ITER, and DEMO. The fabrication process includes inner electrodes out of copper-chromium-zirconium (CuCr1Zr) with a triple helix isolation design, modular vacuum housing consisting of four parts, and additional external coils for electron beam confinement. Detailed assembly procedures are provided for two configurations: the 170 GHz 2 MW coaxial cavity gyrotron and the W7-X upgrade SP gyrotron. The successful manufacturing of the modular collector and a robust design for vacuum tightness are demonstrated. The prototype is now primed for verification in the KIT FULGOR test stand with the W7-X gyrotron for validation of the $E \times B$ drift concept and improvement of the gyrotron efficiency. This comprehensive work bridges theoretical concepts with practical implementation, offering insights crucial for refining and advancing MDCs for megawatt-class gyrotrons for fusion applications.

1 Introduction

The number of magnetically confined fusion research projects is increasing with the aim to achieve an independent, reliable and sustainable energy source. Independent on the confinement device, including stellarators or tokamaks, Electron Cyclotron Resonance Heating (ECRH) systems are considered as key element for heating and stabilisation of the fusion plasma. Gyrotrons are the only known devices capable of producing microwaves at the frequency and power levels required for ECRH. High operational efficiency of gyrotrons is crucial for high ECRH efficiency and reflected in the electrical output power of the fusion power plant.

In vacuum electron tubes, like the gyrotron, an electron beam interacts in the cavity with the electromagnetic wave, however, a considerable amount of power remains in the spent electron beam after the interaction. This power can be partly recovered with a Single-stage Depressed Collector (SDC) to achieve a total gyrotron efficiency of about 50 %. Higher efficiencies are possible with more advanced MDCs. However, traditional MDC designs of other vacuum electron tubes do not work in gyrotrons due to the high magnetic field in the collector region. The most promising concept for electron separation based on their kinetic energy is the $E \times B$ drift concept [1-3]. An MDC prototype with a cylindrical structure and a helical isolation cut was developed and built at KIT [4-6].

2 Fabrication of individual parts

In this section, the fabrication of the individual collector parts is presented divided in the fabrication of the inner electrodes, the vacuum housing and the external magnet coils.

2.1 Fabrication of the inner electrodes

The two electrodes of the MDC are the most important components in the design as their inner surfaces are the only ones represented by the theoretical design which is used for the simulation of electron separation. Other surfaces in the collector are flexible and do not affect the separation of the spent electron beam. CuCr1Zr is used for the electrodes due to the higher mechanical strength in comparison to pure copper. The raw CuCr1Zr of the pre-cut tube for the electrodes, rings for top and bottom of the electrodes and the top plate which connects the second stage with the modular ceramic are shown in Fig. 1(a).

In the first step, the rings were fully machined, heated and put on the pre-machined tube with an interference fit. The rings are additionally secured by screws to the cylinder of the electrodes.

In the second step, a dedicated tool is attached to the top, bottom and inside of the flanged tube for mounting to a Computerized Numerical Control (CNC) machine and stabilization. Then the screw holes for the helical extensions and cooling pipes are machined, followed by

* Corresponding author: benjamin.ell@kit.edu

the gap, separating the first and second electrode. A few bridges in the gap were kept in place until the end of the machining and were removed with hand tools after the complete gap was cut. The machined flanged tube with machined separation gap is shown in Fig. 1(b).

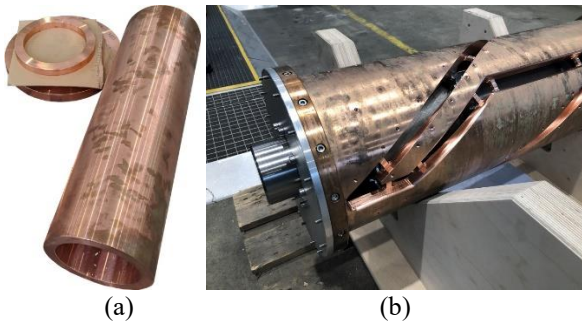


Fig. 1. Raw CuCr1Zr pipe and flanges for the electrodes (a) and machined pipe (b).

In the third step, after the electrodes were separated, the surface in the gap at the positions of the bridges was smoothed out with hand tools. The inner edge of the gap after machining was a sharp 90° edge, as a radius at this position would have required huge effort in programming of the CNC machine and would not have been possible at the positions of the bridges. Fortunately, the separation of the spent electron beam is not sensitive to a specific roundness of the inner edge. However, it is important to reduce the maximum electric field in order to avoid arcing in between the electrodes. The softening of the inner edge was done with hand tools. The finished machined electrodes of the first and second stage are shown in Fig. 2(a) and Fig. 2(b), respectively.

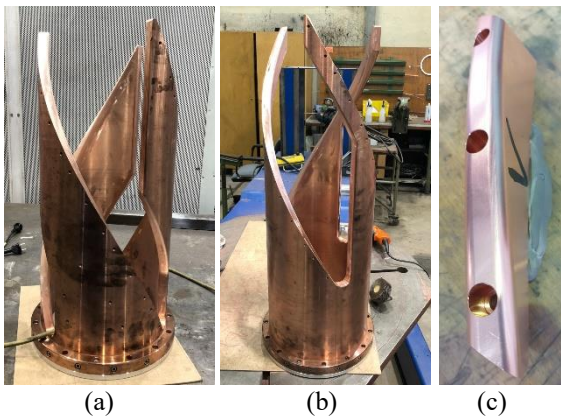


Fig. 2. Finished machined electrodes for the first electrode (a), second electrode (b) and one helical extension (c).

In the fourth step, the modules for extension of the helical surface are pre-cut out of a solid CuCr1Zr block. The pre-cut module is then machined at the surface which mounts to the cylinder of the electrodes together with the holes for mounting. It is then mounted on a dedicated tool to machine the remaining surfaces on a 5-axis CNC machine. The finished module is shown in Fig. 2(c). The MDC SP prototype is a triple helix design with two stages, giving in total six helices. These six helices are divided for the extensions into five modules each, for a total of 30 identical modules. The modules at

top and bottom of a helix are afterwards cut and machined to fit the shape of the cylindrical electrode.

2.2 Fabrication of the vacuum housing

The vacuum housing of the MDC SP prototype consists of four parts: (i) The **lower assembly** which is mounted on top of the mirror-box and supports the first stage of the collector. All cooling and voltage feedthroughs for the first stage are also located in this assembly. (ii) The **middle assembly**, which is mounted on top of the lower assembly and on which the external coils are mounted. (iii) The **modular ceramic**, which is mounted on top of the middle assembly to provide electrical isolation between the gyrotron mirror-box and the second collector stage. (iv) The **top plate**, which is mounted on top of the modular ceramic and connected to the cylindrical part of the second stage.



Fig. 3. Pre-machined stainless steel material for lower and middle assembly.

The lower assembly described here is the version for the KIT 2 MW 170 GHz coaxial-cavity gyrotron for demonstration of the more complicated fabrication process. The lower assembly for the W7-X upgrade SP gyrotron is much smaller and milled out of a solid block of stainless steel. Majority of the material for the lower and middle assembly are shown in Fig. 3. Both cylindrical parts are produced by rolled and welded sheets of stainless steel, which is machined on a lathe to achieve the desired accuracy.

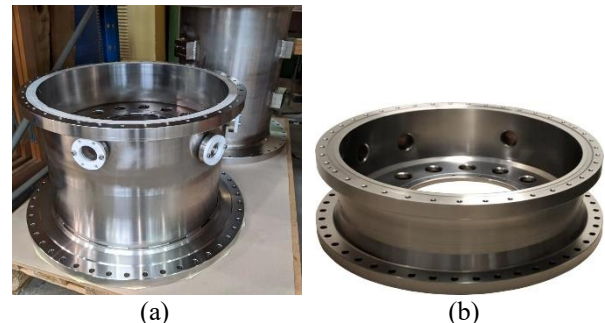


Fig. 4. Machined lower assembly for KIT 2 MW 170 GHz coaxial-cavity gyrotron (a) (foreground) middle assembly (a) (background) and lower assembly for W7-X gyrotron (b).

In the first step, the pre-machined flanges are welded on the ends of both cylinders. In the second step, the sealing edges and screw holes of the flanges are machined to ensure correct planar alignment between top and bottom of the cylinder. In the third step,

additional feedthroughs, mounting blocks and the finished machined intermediate floor of the lower assembly are welded in place. Both versions of the finalized lower assemblies and the finalized middle assembly are shown in Fig. 4(a) and Fig. 4(b).

2.3 Fabrication of the coil assembly

Three additional external magnet coils are required for the MDC SP prototype to modify the spent electron beam inside the $E \times B$ region to a constant beam radius. The coils will be operated with a constant current, hence no eddy currents are induced in the winding body of the coil during operation. A non-slotted aluminium winding body was chosen for all coils. On the outer side of the winding body are screw holes to mount brackets for fixation of the coils to each other and to the middle assembly as well as lifting brackets for easier handling during assembly. The electrical connection of the coils is realized with commercially available ceramic clamps on the side of the coils. Winding of the coils was done on a dedicated winding machine for a dense packaging of the rectangular copper wire. A summary of the coil winding processes with the correct number of turns per layer is given in Tab. 1. The maximum operation temperature of the coils is at 200°C, due to the insulation coating on the individual wires. Additional cooling jackets have been produced to increase the operation time of the coils. A finished coil is shown in Fig. 5(a) and a cooling jacket is shown in Fig. 5(b).



Fig. 5. One of three external coils (a) and cooling jacket for increased operation time (b).

Table 1. Number of turns per layer and total number of turns for each coil.

Layer	Coil A	Coil B	Coil C
1	28.25	28.25	28.75
2	28.25	28.00	27.50
3	28.31	28.19	28.75
4	28.31	28.19	28.50
5	28.50	28.00	28.50
6	28.00	28.19	28.75
7	28.04	28.00	28.75
8	28.00	28.50	28.25
9	28.00	-	-
10	28.00	-	-
11	28.00	-	-
12	28.00	-	-
13	28.00	-	-
14	29.00	-	-
total	394.65	225.33	227.75

3 Assembly of the prototype

Two different assemblies of the MDC SP prototype have been done until end of 2023 and are presented in

the next two subsections. The first assembly of the vacuum housing is in a configuration for the KIT 2 MW 170 GHz coaxial-cavity gyrotron, while the second assembly of the complete collector is in a configuration for the W7-X upgrade SP gyrotron.

3.1 Assembly of the vacuum housing in 2 MW coaxial-cavity gyrotron configuration

The first assembly was done after all components for the vacuum housing and the external coils were fabricated. This includes a cover flange for the bottom to seal the collector and pump vacuum without a gyrotron attached to it, the lower assembly for the KIT 2 MW 170 GHz coaxial-cavity gyrotron, the middle assembly, the modular ceramic, the top plate and the coils. The electrodes and the lower assembly for the W7-X upgrade SP gyrotron were not finished at this stage and therefore not included in the first assembly. No internal components were mounted in the housing, significantly simplifying the process. The individual components were installed from bottom to top, starting with cover flanges to the bottom and feedthrough flanges of the lower assembly. Next, the middle assembly was mounted on the lower assembly as shown in Fig. 6(a), followed by the modular ceramic and the top plate to close the vacuum housing as shown in Fig. 6(b).

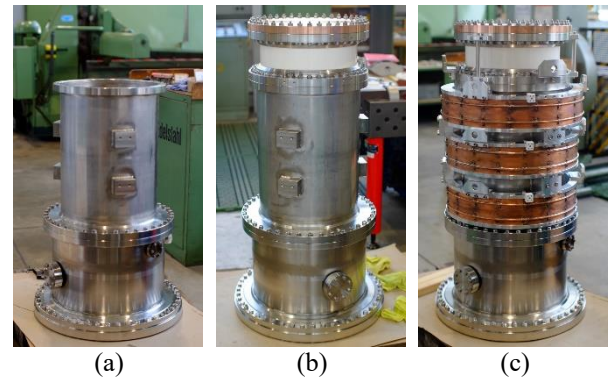


Fig. 6. Assembly of the vacuum housing in 2 MW coaxial-cavity gyrotron configuration.

The assembly of the external parts started with mounting the lifting brackets to the coils and combining them with the mounting brackets to a single assembly. The coil assembly was then lifted over the vacuum housing and lowered to the support mounts on the middle assembly. In the final step, the transport protection was put on the ceramic and the lifting brackets for the complete collector were mounted on the bottom flange of the modular ceramic. It is important to note that the lifting of the collector is only supported by these lifting brackets and not from any point above the ceramic to avoid damage to the ceramic. The process of assembly of the vacuum housing and external parts proceeded as planned without interruptions due to incorrectly produced parts. The partly assembled collector achieved an excellent vacuum leaking rate of under 1.0×10^{-12} mbar·l·s⁻¹ (limitation of the measurement device) at a pressure of 1.1×10^{-7} mbar after pumping. The closed vacuum housing is shown in Fig. 6(c).

3.2 Assembly of the complete MDC in W7-X upgrade SP gyrotron configuration

The second assembly of the MDC SP prototype was done after all parts were fabricated. This time the second version of the lower assembly was used to make the collector compatible with the W7-X upgrade SP gyrotron at KIT. It is currently planned to make the world's first MDC experiments with a fusion relevant gyrotron with this tube due to the availability of equipment. The MDC can only be operated with the modular power supply from AMPEGON in the new Fusion Long Pulse Gyrotron Laboratory (FULGOR) test stand at KIT. Experiments at the old KIT gyrotron test stand are currently not possible, as no high voltage connection between both test stand exist. The FULGOR test stand was designed with cryogen free magnets in mind, limiting the available experimental equipment further. The next available cryogen free magnet at the FULGOR test stand is a 4.5 T magnet from Commissariat à l'énergie atomique et aux énergies alternatives (CEA) Tungsten (chemical symbol "W") Environment in Steady-state Tokamak (WEST) and it is possible to operate the W7-X upgrade SP gyrotron in this magnet at 105 GHz.

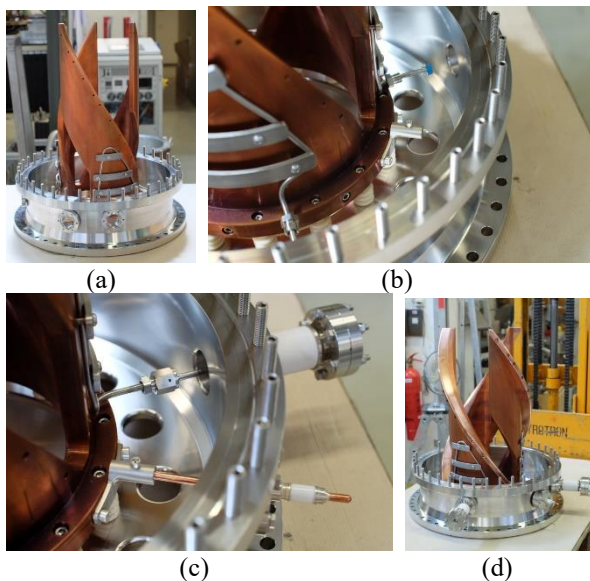


Fig. 7. Assembly of the first electrode in W7-X upgrade configuration.

The second assembly started with the lower assembly and the ceramic insulators of the first stage which are screwed onto the intermediate floor. Then the cylindrical part of the first electrode is lowered on the insulators and fixed with screws. In the next step, the cooling pipe is mounted on the outside of the first electrode and the mount for the high voltage connection is mounted on the bottom flange of the electrode. Snapshots of the assembly progress are shown in Fig. 7(a) and Fig. 7(b). Finally, the feedthroughs, as shown in Fig. 7(c), and helical extensions are mounted to the first electrode, finalizing this part of the MDC. The completed first electrode is shown in Fig. 7(d).

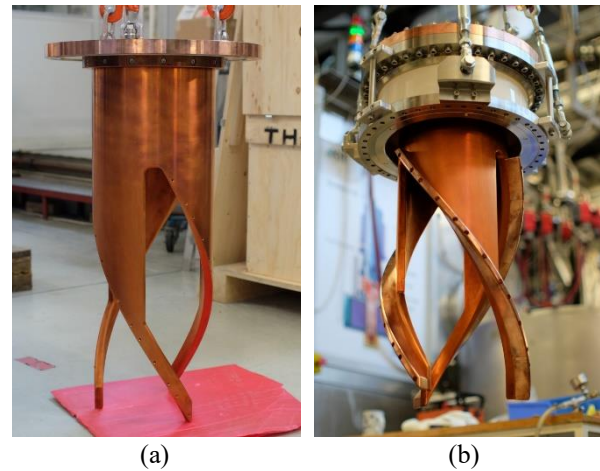


Fig. 8. Assembly of the second electrode.

Assembly of the second electrode started with mounting the top plate to the cylindrical part of the second electrode, as shown in Fig. 8(a). In the next step, the anti-corona ring was mounted inside at the lower flange of the modular ceramic to avoid increased electric field at the welded metal which connects the ceramic to the metal flanges. Then the cylindrical part of the second electrode was lowered through the modular ceramic and the top flanges were bolted together. In the final step of assembly of the second electrode, the helical extensions are mounted on the outside of the cylinder. The final step was performed in this order to allow a smaller ceramic to be made to provide potential isolation for the second collector stage. The finished assembly of the second electrode is shown in Fig. 8(b).

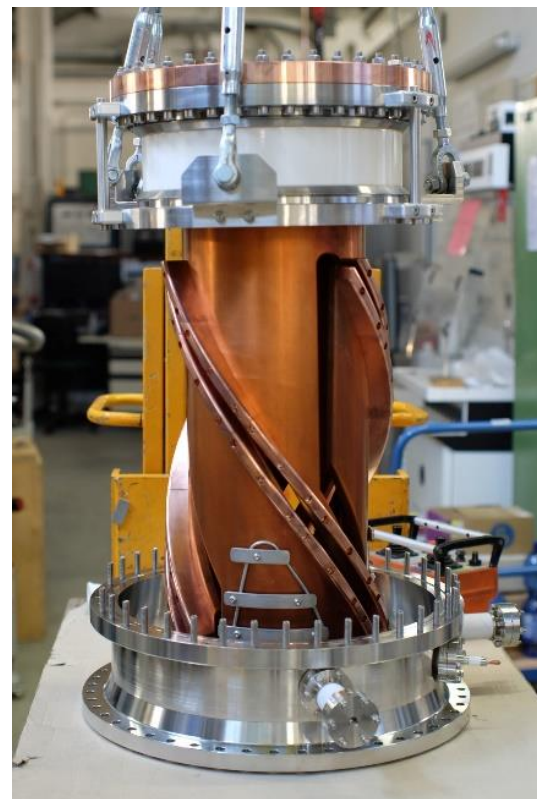


Fig. 9. Assembly demonstration of both electrodes without vacuum housing.

The final step in assembly of the MDC electrodes is the combination of both electrode assemblies as shown in Fig. 7(d) and Fig. 8(b) with the middle assembly of the vacuum housing. To demonstrate the fit of both electrodes and to train for the final and most complicated assembly step, an assembly test without the vacuum housing was performed. Note that due to the extension of the helical gap in axial direction, the second electrode must be rotated as it is lowered to avoid collision with the first electrode and potential damage. A view of the MDC electrodes without the vacuum housing is shown in Fig. 9. The assembly test and the process of simultaneous lowering and rotation of the second electrode was successfully practised.

The easiest approach to continue with the last step in the assembly process is to mount the middle assembly on the lower flange of the modular ceramic and lower the part onto the assembly with the first electrode. The process of rotation as the upper part of the MDC is lowered to the lower part is documented in a few time steps in Fig. 10(a)-(c). The assembly process was considered during the mechanical design of the MDC SP prototype and the middle assembly of the vacuum housing was deliberately made shorter than the second electrode to allow it to be viewed from the side when lowered. The lower tip of the second electrode is best visible in Fig. 10(a) for two different azimuthal positions. A view from the bottom of the assembled MDC SP prototype is shown in Fig. 10(d). The collector bottom was closed with a flange at the bottom to pump vacuum and keep the internal parts of the collector clean while waiting for the experimental equipment to become available.

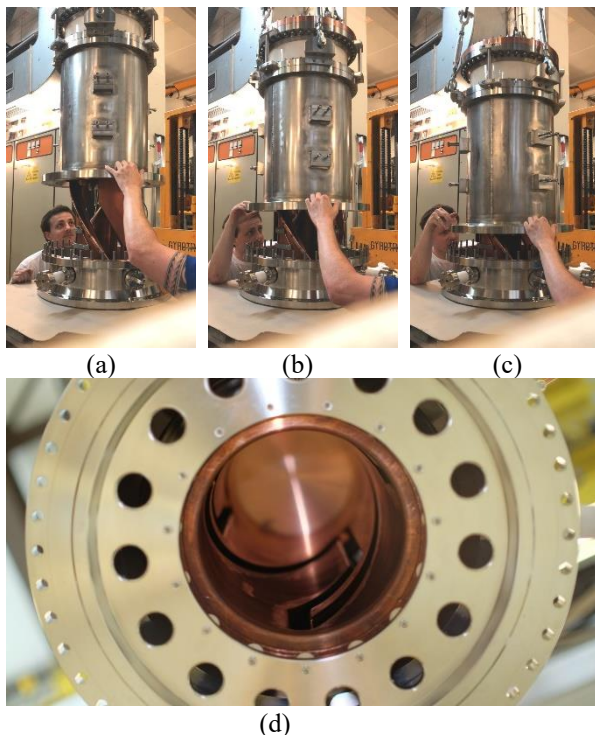


Fig. 10. Closing of the vacuum housing with electrodes (a), (b) and (c). Few from the bottom of the assembled MDC prototype (d).

4 Conclusion

The fabrication and assembly of the MDC SP prototype has been carried out successfully at KIT. The prototype is ready for verification in the KIT FULGOR test stand with the next available gyrotron. The work provides a valuable guideline for future modifications and improvements in this innovative field of research.

This work has been carried out within the framework of the EUROfusion Consortium, funded by the European Union via the Euratom Research and Training Programme (Grant Agreement No 101052200 — EUROfusion). Views and opinions expressed are however those of the author(s) only and do not necessarily reflect those of the European Union or the European Commission. Neither the European Union nor the European Commission can be held responsible for them.

References

1. I. Gr. Pagonakis, J.-P. Hogge, S. Alberti, K. A. Avramides, J. L. Vomvoridis, A new concept for the collection of an electron beam configured by an externally applied axial magnetic field. *IEEE Trans. on Plasma Sci.* **36**, 469-480 (2008).
<https://doi.org/10.1109/TPS.2008.917943>
2. C. Wu, I. Gr. Pagonakis, S. Illy, G. Gantenbein, M. Thumm, J. Jelonnek, Comparison between controlled non-adiabatic and E×B concepts for gyrotron multistage depressed collectors. *EPJ Web of Conf.* **149**, 04005 (2017).
<https://doi.org/10.1051/epjconf/201714904005>
3. V. N. Manuilov, M. V. Morozkin, O. I. Luksha, M. Yu Glyavin, Gyrotron collector systems: Types and capabilities. *Infrared Phys. Tech.* **91**, 46-54 (2018).
<https://doi.org/10.1016/j.infrared.2018.03.024>
4. C. Wu, I. Gr. Pagonakis, K. A. Avramidis, G. Gantenbein, S. Illy, M. Thumm, J. Jelonnek, Gyrotron multistage depressed collector based on E×B drift concept using azimuthal electric field. I: Basic design. *Phys. of Plasmas* **25**, 033108 (2018).
<https://doi.org/10.1063/1.5016296>
5. C. Wu, I. Gr. Pagonakis, D. Albert, K. A. Avramidis, G. Gantenbein, S. Illy, M. Thumm, J. Jelonnek, Gyrotron multistage depressed collector based on E×B drift concept using azimuthal electric field. II: Upgraded designs. *Phys. of Plasmas* **26**, 013108 (2019).
<https://doi.org/10.1063/1.5078861>
6. B. Ell, C. Wu, G. Gantenbein, S. Illy, M. Misko, I. Gr. Pagonakis, J. Weggen, M. Thumm, J. Jelonnek, Toward the first continuous wave compatible multistage depressed collector design for high power gyrotrons. *IEEE Trans. on Elec. Devices* **70**, 1299-1305 (2023).
<https://doi.org/10.1109/TED.2023.3234885>